JTTEE5 8:393-398

Peer Reviewed

The Modeling of Coating Thickness, Heat Transfer, and Fluid Flow and Its Correlation with the Thermal Barrier Coating Microstructure for a Plasma Sprayed Gas Turbine Application

P. Nylén, J. Wigren, L. Pejryd, and M.-O. Hansson

(Submitted 18 August 1998; in revised form 11 February 1999)

The plasma spray deposition of a zirconia thermal barrier coating (TBC) on a gas turbine component was examined using analytical and experimental techniques. The coating thickness was simulated by the use of commercial off-line software. The impinging jet was modeled by means of a finite difference elliptic code using a simplified turbulence model. Powder particle velocity, temperature history, and trajectory were calculated using a stochastic discrete particle model. The heat transfer and fluid flow model were then used to calculate transient coating and substrate temperatures using the finite element method. The predicted thickness, temperature, and velocity of the particles and the coating temperatures were compared with these measurements, and good correlations were obtained. The coating microstructure was evaluated by optical and scanning microscopy techniques. Special attention was paid to the crack structures within the top coating. Finally, the correlation between the modeled parameters and the deposit microstructure was studied.

Keywords coating thickness, deposit heat transfer, fluid flow, modeling, plasma spraying

1. Introduction

Plasma spraying has been used to produce high performance metallic and ceramic coatings for many years and is currently used in a number of areas within the manufacturing industry. However, even after over thirty years of use, the process is still highly empirical. Theoretical modeling has in recent years given a better scientific understanding and increased coating performance. Several models have been presented in various papers for predicting coating thickness (Ref 1-4), predicting plasma and inflight particle temperatures (Ref 5-9), and predicting deposit and substrate temperatures (Ref 10, 11). These models are limited to creating robot trajectories and predicting coating/substrate temperatures on noncomplex part geometries. The objective of this on-going modeling work is to develop a tool for the engineer where coating thickness and temperatures can be predicted and optimized on complex part geometries. This article presents the assumptions and principles behind the modeling techniques and an evaluation of the correlations between modeled and measured parameters. The correlation between modeled parameters and the top coat microstructure is of particular interest. This study was carried out on a gas turbine component sprayed with a partially stabilized zirconia powder using an Ar-H_2 atmospheric plasma jet.

The modeling can be divided into the following components: (a) coating thickness prediction by the use of off-line programming (OLP) techniques, (b) modeling of the impinging plasma jet and plasma-particle interactions, and (c) heat transfer modeling between the plasma jet and workpiece.

2. Coating Thickness Prediction and Robot Trajectory Generation

In this study, programming was based on a simulation of the process used by the IGRIP system of Deneb Robotics Inc. (Auburn Hills, MI). The model consisted of three main parts: (a) a geometric, kinematic, and dynamic model of the robot, (b) a model of the workpiece to be sprayed, and (c) a model for the distribution of the particles, that is, the spray cone. The simulation was preceded by building a geometric model of the surface to be coated. The mathematical B-spline (Ref 12) representation was used. An empirical model of the spray cone was defined by spraying a test plate in two perpendicular directions and measuring the coating thickness distributions in these two directions. A robot trajectory was generated by defining gun locations and

This paper originally appeared in *Thermal Spray: Meeting the Challenges of the 21st Century; Proceedings of the 15th International Thermal Spray Conference*, C. Coddet, Ed., ASM International, Materials Park, OH, 1998. This proceedings paper has been extensively reviewed according to the editorial policy of the *Journal of Thermal Spray Technology.*

P. Nylén, University Trollhättan/Uddevalla, Box 957, S-461 29 Trollhättan, Sweden; and **J. Wigren, L. Pejryd,** and **M.-O. Hansson,** Volvo Aero Corporation S-461 81 Trollhättan, Sweden. Contact e-mail: per.nylen@thn.htu.se.

Peer Reviewed

orientations. The trajectory was simulated, and the coating thickness was calculated by a coating simulator, which calculated the interaction of the spray cone with the surface. In the calculations the surface to be coated was approximated by triangles and the thickness predicted for each surface triangle. The coating thickness was finally analyzed and the spray path optimized. Reference 13 gives a more detailed description of OLP systems and thickness modeling techniques.

3. The Modeling of Plasma Jet and Plasma-Particle Interactions

Modeling energy transport in a thermal plasma jet requires solving equations for mass, momentum, and energy conservation. The developed model is based on the following assumptions:

- Identical gases in the jet and the surroundings
- Axisymmetric jet
- Neglected radiation losses from the gas/plasma
- Isotropic materials
- Turbulent flow
- Negligible body forces
- Negligible chemical reactions in the jet and between the jet and the surroundings
- Newtonian fluid

The plasma was represented as an ideal gas with temperature-dependent thermodynamic and transport properties. The governing equations were solved by a finite-difference scheme (Ref 14). A Prandtl model (Ref 14) was used to model the effects of turbulence, which adds a turbulent viscosity and conductivity. In order to calculate particle trajectories, temperature histories and distributions of particle impact temperatures, positions, and velocities, a stochastic two-dimensional model was used. This model was based on the following assumptions:

- A two-dimensional plasma flow in which particles maintain axial and radial trajectories
- Spherical particles
- Local thermodynamic equilibrium (LTE)
- Optically thin plasma
- Negligible gravitational effects
- Negligible effects of thermophoresis (Ref 9), Basset history (Ref 9), and particle charging
- Negligible turbulent effects on particle trajectories

Corrections of the fluid properties of viscosity, density, and conduction, due to strongly varying properties through the boundary layer, were carried out by calculating the mean integral values as proposed by Bourdin et al. (Ref 15). The partial differential equation for heat conduction in spherical coordinates (Ref 16) was solved by a finite difference scheme to give the thermal history of the powder particles. This takes into account convective and radiative heat transfer (radiative heat transfer from the plasma to the particles is, however, neglected), phase changes, and vaporization. Noncontinuum effects were considered by adjusting the viscous drag and Nusslets number as proposed by Pfender and Lee (Ref 8). The particles were modeled as discrete Lagrangian entities that exchange momentum and energy with the plasma. When calculating these interactions it is assumed that the particle loading effect on the plasma is negligible, that is, the presence of particles will have little effect on gas velocities and temperatures. Each particle in the model represented a group of similar particles, N_p. Particles were generated with normal distributed sizes, injection points, injection velocities, and temperatures in relation to a given particle loading rate. Reference 17 gives a more detailed description of the plasma and particle model.

4. The Modeling of Heat Transfer in the Substrate and Deposit

It is assumed that the plasma gas exits the nozzle with a uniform velocity and temperature and that there is thermal and compositional equilibrium with the ambient. The heat transfer from the arc to the substrate can be written:

$$q_f = h_f(T_f - T_s) + q_{rad} \quad \text{(Eq 1)}$$

where q_{rad} is the radiative transfer from the plasma to the target and q_f is the total heat flux from the plasma jet to the substrate. Previous calculations by Nylen and Edberg (Ref 17) showed that the radiative heat transfer q_{rad} in Eq 1 can be neglected. The heat transfer coefficient, h_f, in Eq 1 is derived from the Nusselt number, which in turn is derived from empirical data from impinging gas jets (Ref 18). The heat transfer from the particles to the substrate can be written:

$$q_p = h_p(T_p - T_s) \quad \text{(Eq 2)}$$

where h_p is the thermal resistance (Ref 19) between the particles and the substrate. The total heat flux to the substrate is then calculated by:

$$q_{in} = q_f + q_p \quad \text{(Eq 3)}$$

The heat flux from the substrate and deposit is similarly assumed to have a convection part and a radiation part:

$$q_{out} = h(T_p - T_s) + \varepsilon(T_p - T_s)^4 \quad \text{(Eq 4)}$$

The temperature distribution in the object as a function of time was then calculated by the finite element method (FEM). Numerical solutions were obtained by using the ANSYS program (Ref 20), employing a series of increments and iterating in each increment to obtain equilibrium.

5. Experimental Procedures

A gas turbine component (Fig. 1) was sprayed and evaluated to verify the modeling work. In Fig. 1, one-quarter of the ring was cut out to reveal the cross section.

5.1 Materials

Commercially available powders were used in this study. The NiCrAlY bond coat was produced by Praxair Inc. (Indianapolis, IN) as Ni211, and the 8% yttria partially stabilized zirconia top coat was produced by H.C. Starck (Germany) as Amperit 827. The top coat powder size was –75 + 20 μm.

5.2 Plasma Spraying

Plasma spraying was carried out using the F4 gun from Sulzer Metco (Westbury, New York) controlled from a Sulzer Metco A3000S system (automated, robotized, etc.). The coating was applied by means of plasma spraying with the powder injected radially 6 mm downstream from the nozzle. A six layer bond coat to a total thickness of 120 μm and a 25 layer top coat to a total thickness of 1075 μm were applied. The plasma jet was a mixture of argon and H_2 with a total flow rate of 36 slpm and a 52 slpm bond coat and top coat, respectively. The power levels of the torch were 40 and 52 kW, respectively. The component to be sprayed was mounted on a rotational table. The speed of the rotational table was adjusted to maintain a torch/surface relative velocity of 75 m/min. The deposits were cooled during spraying with an air jet. The component was preheated. The spraying distance was kept constant (120 mm for the bond coat, 85 mm for the top coat). Six points along the surface normal defined the robot trajectory.

5.3 Metallography

Metallography was performed according to standard practices using vacuum mounting techniques and automatic polishing with Struers Prepamatic equipment (Struers Inc., Copenhagen, Denmark). Long polishing times were performed to reveal the true microstructure, which was evaluated using light optical microscopy. A point counting procedure was used to quantify the microstructure.

5.4 Diagnostics

Diagnostics of inflight sprayed particles were made using the optical system DPV2000 (Tecnar Inc., Montreal, Canada). This system is based on the detection of thermal radiation of the hot sprayed particles by an optical sensor located perpendicular to the spray jet and consisting of a focusing lens and optical fibers (Ref 20, 21). The DPV2000 measures parameters (velocity, temperature, and size) of inflight particles in the measurement volume of 200 by 300 μm by 2.5 mm along the optical axis (Ref 21).

5.5 Surface Temperatures

Surface temperatures were measured by two thermocouples at the rear side of the component (Fig. 2). To estimate the thermal resistance, a pyrometer simultaneously measured the temperature history at the coating surface, located opposite from one of the thermocouples.

6. Results

The modeling and measurement results were restricted to the top coat. The OLP system IGRIP was used to simulate the coating thickness. Figure 3 presents simulated and measured thickness values.

In the temperature simulations of the plasma jet, properties of the argon-hydrogen gas mixture were taken from the computer program ADEP (University of Limoges, Limoges Cedex, France) (Ref 22). Figures 4 and 5 show simulated velocity and temperature center line values. The simulated velocity and temperature distributions of the particles at a distance of 65 mm (origin is located on the nozzle center line) in Fig. 6 and 7 compare extremely well with the inflight measurements in Table 1.

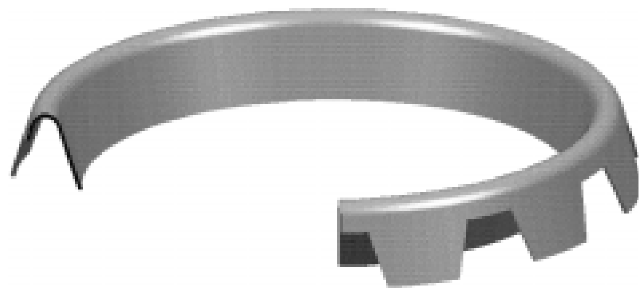

Fig. 1 Gas turbine component. The diameter of the ring is 320 mm.

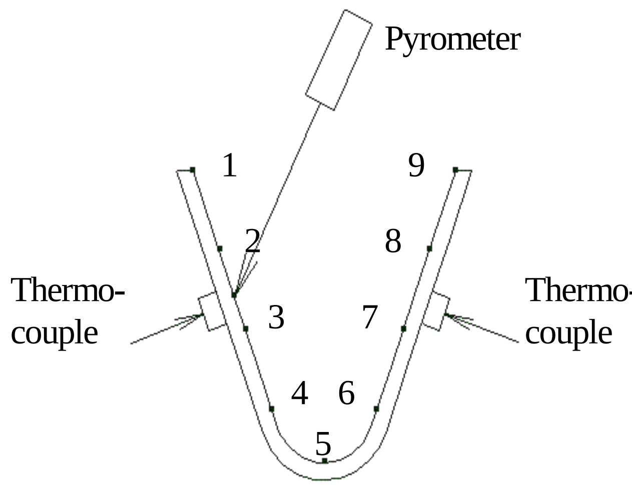

Fig. 2 Location of pyrometer and thermocouples

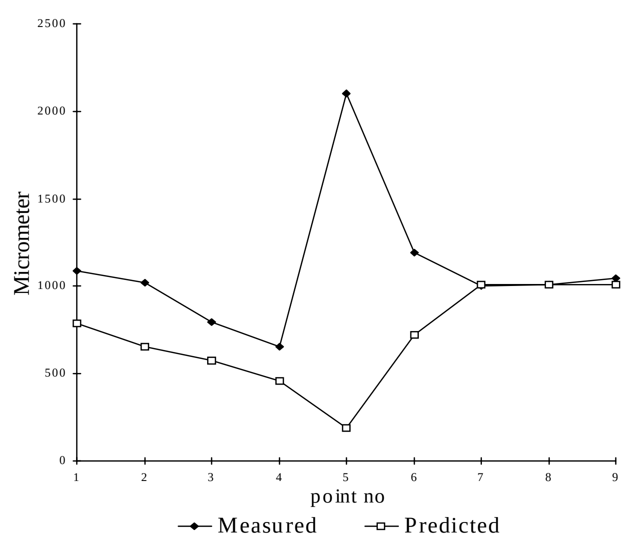

Fig. 3 Simulated and measured top coat thickness (μm)

Figure 8 shows the pyrometer temperature history. These temperatures should be compared with the simulated temperatures in Fig. 9. In Fig. 9 the temperature history in the bottom region (point 5 in Fig. 2) is also given. The temperatures are approximately 50° lower in the bottom region. In the microstructural evaluation the coating was divided into two different regions: a side region (points 1 to 3 in Fig. 2) and a bottom region (points 4 to 6 in Fig. 2). As can be seen in Fig. 10 and 11, the microstructure is different in these two regions. The amount of vertical microcracks is the same, ~1.5/mm, but the porosity is quite different. Porosity is in the range of 7%, and more randomly distributed in the side region (Fig. 10), while it is higher and with a marked linearity in the bottom region of the part (Fig. 11). This linearity is periodical with a more marked appearance at the bottom of the third, fifth, seventh, and so on, gun pass; a less marked appearance is visible at the bottom of the second, fourth, sixth, and so on, gun pass. The coating is also about twice as thick in the bottom region as on the side.

Table 1 Simulated and measured particle properties

Average properties in a point 65 mm down stream at center of flux	Measurements	Model
Velocity	167 m/s	175 m/s
Temperature	3473 K	3425 K
Size	32 µm	44 µm

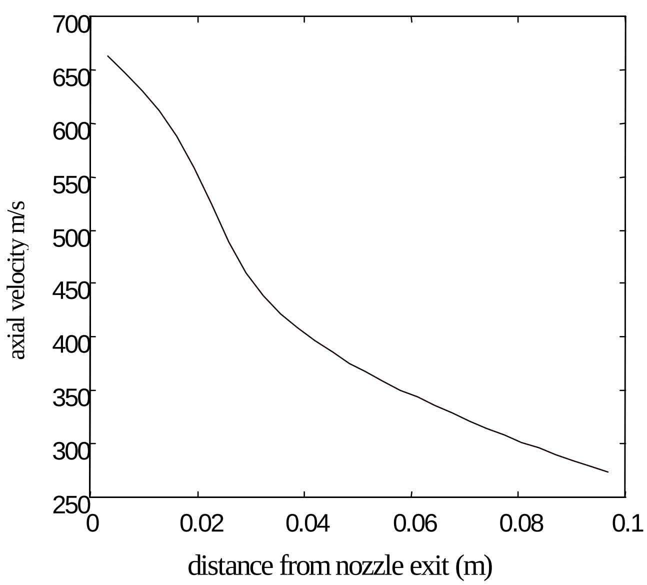

Fig. 4 Simulated centerline velocities of the jet

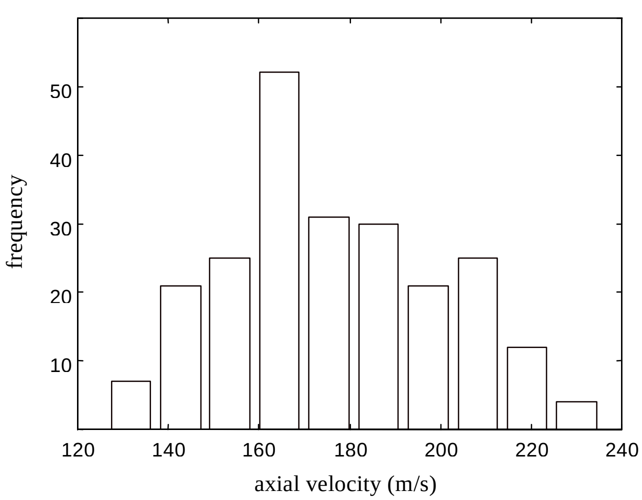

Fig. 6 Simulated axial particle velocities 65 mm from nozzle exit

7. Discussion

One explanation for the thickness difference between the predicted and measured values in the bottom region (points 4 to 6 in Fig. 2) is probably due to bad adhesion at the sides (points 1 to 3 and 7 to 9 in Fig. 2). The adhesion effect is currently not included in the model. The higher measured values in the bottom

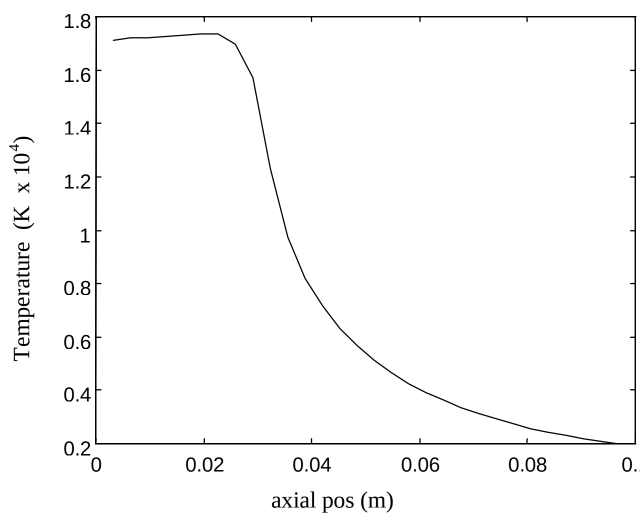

Fig. 5 Simulated centerline temperatures of the jet

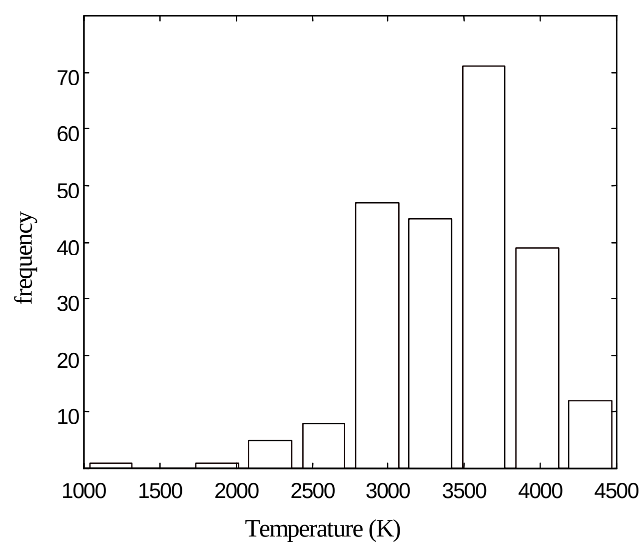

Fig. 7 Simulated particle surface temperatures 65 mm from nozzle exit (K)

region are likely derived from the fact that unmelted particles do not adhere to the side surfaces. They will, to some extent, exist in the bottom of the component and, thereby, become incorporated in the coating when the spray cone passes that area. The difference also depends on the robot acceleration, which probably is higher in the model. The programmed gun traverse speed was 40× higher in the bottom region. The acceleration limits of the robot were, however, not able to achieve such accelerations. However, the major reason for the discrepancy between the measured and predicted values is probably due to simulation errors, such as poor calculation of the thickness when spraying at a steep angle to the surface. Because rotational symmetry is not considered in the calculations, a more rational model could also be developed. The model could incorporate a more sophisticated thickness calculation method, where adhesion effects are considered.

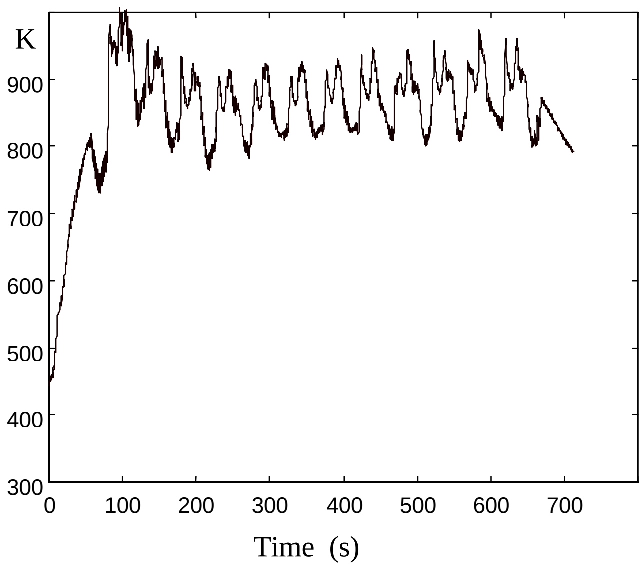

Fig. 8 Coating temperature history (pyrometer)

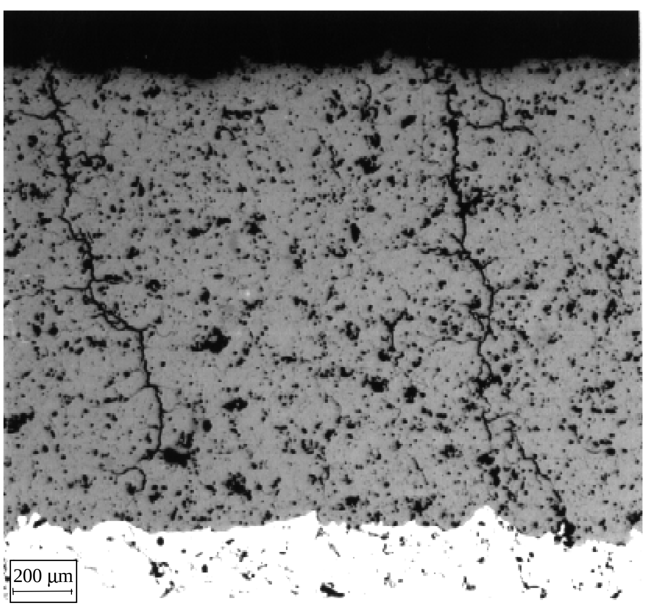

Fig. 10 Microstructure of the 1 mm thick thermal barrier coating at the side region (points 1 to 3 in Fig. 2)

The particle inflight simulations gave very good agreement with the measurements. However, a more extensive modeling and measurement study would need to be conducted to determine whether interaction phenomena, such as loading and turbulence effects on particle trajectories, should be considered.

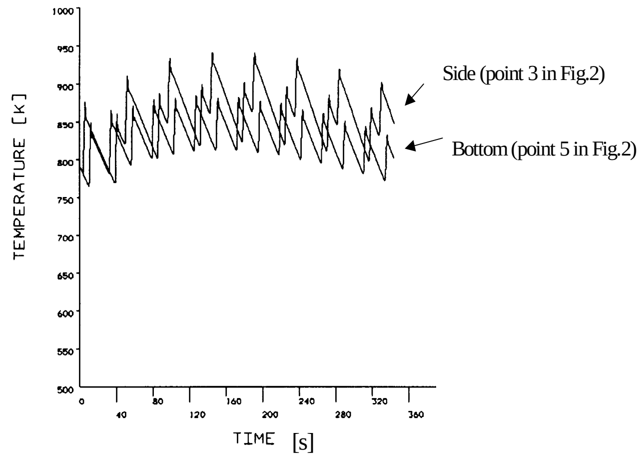

Fig. 9 Calculated temperature histories in point 3 (side) and point 5 (bottom) nodes in Fig. 2

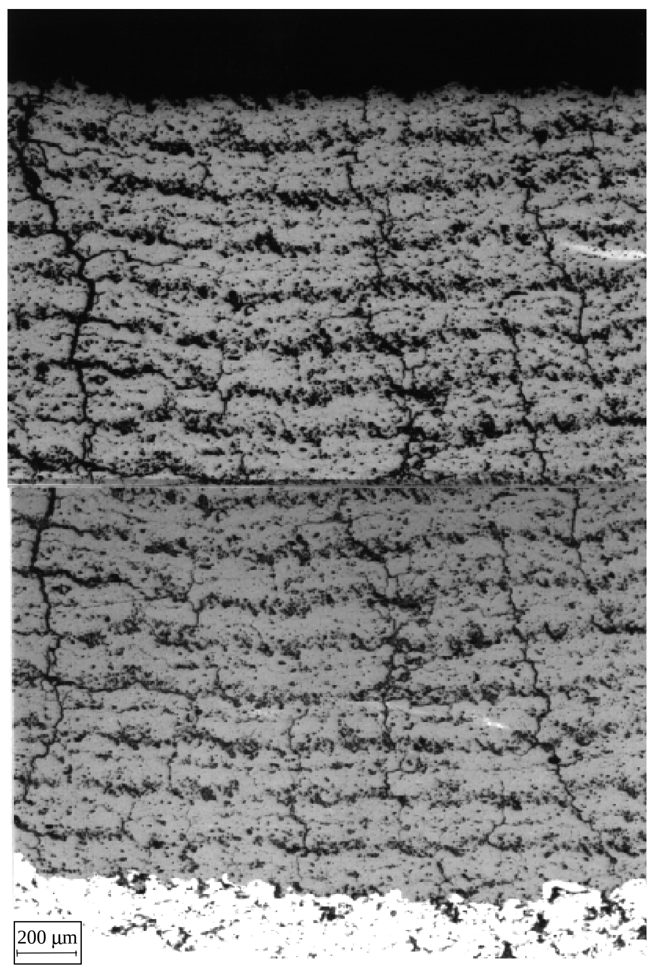

Fig. 11 Microstructure of the 2 mm thick thermal barrier coating at the bottom region (points 4 to 6 in Fig. 2)

Peer Reviewed

In the coating/substrate temperature modeling, the temperature levels were adjusted because it was difficult to estimate the heat transfer coefficients (h in Eq 4) at the surface and rear side of the part. The thermal contact resistance is also difficult to calculate. The method described, with simultaneous thermocouple and pyrometer measurements, therefore, is necessary. The modeling showed that the temperature during spraying (Fig. 9) is in all cases higher than 400 °C. Vertical segmentation cracks were found in all areas of the component. Bengtsson (Ref 23) has shown that temperatures of 400 °C produced desired vertical segmentation cracks. The particle surface temperature simulation predicted 13% unmelted particles. If the core temperature had been calculated instead, this amount would have probably increased substantially. The high porosity evaluated in the bottom region is likely to come from these downfallen particles.

7. Conclusions

In this article, models simulating coating thickness, fluid flow and temperature in the plasma jet, particle temperatures, velocities, and heat transfer in the deposit and substrate have been evaluated, and good agreements with measurements were found. The correlation between modeled parameters and a top coat microstructure was tentatively evaluated. Further studies linking these parameters would be valuable.

Acknowledgments

The authors wish to acknowledge the metallographic work of Fredrik Almroth, the OLP work of Ingemar Fransson, and the financial support of Stiftelsen för Kunskaps och Kompetensutveckling, project No. 1996/654.

References

1. G. Goedjen, R. Miller, and W. Brindley , " A Simulation Technique for Predicting Thickness of Thermal Sprayed Coatings," NASA Army Research Laboratory Technical Report, ARL-TR-762, 1995
2. F. Mikosch, *Precise Manufacturing with Off-Line Programmed Robots Integration in Manufacturing Enables Innovative Robotics Solutions,* ESPRIT project No. 6457, 1995, p 331-340
3. S. Cirolino, J.H. Harding, and G. Jacucci, Computer Simulation of Plasma-Sprayed Coatings I. Coating Deposition Model, *Surf. Coat. Technol.,* Vol 48, 1991, p 137-145
4. M. Fasching, F. Prinz, and L.E. Weiss, Planning Robotic Trajectories for Thermal Spray Shape Deposition, *J. Therm. Spray Technol.,* Vol 2, 1993, p 45-50
5. J. Szekely and R.C. Westhoff, Recent Advances in the Mathematical Modeling of Transport Phenomena in Plasma Systems, *Thermal Plasma Applications in Materials and Metallurgical Processing,* 1992, p 55-72
6. C.H. Chang, Numerical Simulation of Alumina Spraying in Argon-Helium Plasma Jet, *Thermal Spray: International Advances in Coatings Technology,* C.C Berndt, Ed., ASM International, 1992, p 793-798
7. M. Vardelle, A. Vardelle, P. Fauchais, and M. Boulos, Plasma-Particle Momentum and Heat Transfer: Modeling and Measurements, *AIChE J.,* Vol 29 (No. 2), 1983, p 236-243
8. E. Pfender, Particle Behaviour in Thermal Plasmas, *Plasma Chem. Plasma Process.,* Vol 9 (No. 1) (supplement), 1989, p 167-195
9. E. Pfender and Y.C. Lee, Particle Dynamics and Particle Heat and Mass Transfer in Thermal Plasmas. Part I. The Motion of a Single Particle without Thermal Effects, *Plasma Chem. Plasma Process,* Vol 5 (No. 3), 1985, p 211-237
10. O. Knotek, U. Balting, T. Cosack, and P. Pantucek, Measurements and Mathematical Modelling of Heat Flow into Substrates during Atmospheric Plasma Spraying of Coated Compounds as a Starting Point for Strain Calculations, *Second Plasma Technik Symposium,* Vol 1, 1991, p 103-110
11. H. Leyers, H. Adamietz, H. Sbuchkremer, and D. Stöver, Heat Transport between Plasma Jet and Workpiece in Plasma Spraying, *Second Plasma Technique Symposium,* Vol 1, 1991, p 111-121
12. D.F. Rogers and J.A. Adams, *Mathematical Elements for Computer Graphics,* McGraw Hill, 1990
13. P. Nylén, I. Fransson, A. Wretland, and N. Martensson, Coating Thickness Prediction and Robot Trajectory Generation of Thermal Sprayed Coatings, *Thermal Spray: Practical Solutions for Engineering Problems,* C.C. Berndt, Ed., ASM International, 1996, p 693-698
14. B.R. Munson, D.F. Young, and T.H. Okiishi, *Fundamentals of Fluid Mechanics,* John Wiley & Sons, 1994
15. E. Bourdin, P. Fauchais, and M. Boulos, Transient Heat Conduction under plasma conditions, *Int. J. Heat Mass Transfer,* Vol 26, 1983, p 567-582
16. F.P. Incropera and D. De Witt, *Fundamentals of Heat and Mass Transfer,* John Wiley & Sons Inc., 1990
17. P. Nylén and M. Edberg, Robot Trajectory Generation and Coating Temperature Prediction of Plasma Sprayed Coatings, *Thermal Spray: A United Forum for Scientific and Technological Advances,* C.C. Berndt, Ed., ASM International, 1997, p 583-592
18. H. Martin, Heat and Mass Transfer between Impinging Gas Jets and Solid Surfaces, *Advances in Heat Transfer,* Vol 13, J.P. Hartnett and T.F. Irvine, Jr., Ed., Academic Press, 1977, p 1-51
19. *ANSYS Reference Manual,* Version 5.0, Swanson Analysis Systems Inc., 1992
20. C. Moreau, P. Gougeon, M. Lamontagne, V. Lacasse, G. Vaudreuil, and P. Cielo, On-Line Control of the Plasma Spraying Process by Monitoring the Temperature, Velocity, and Trajectory of In-Flight Particles, *Thermal Spray: Industrial Applications,* C.C. Berndt and S. Sampath, Ed., ASM International, 1994, p 431-437
21. P. Gougeon, C. Moreau, V. Lacasse, M. Lamontagne, I. Powell, and A. Bewsher, Advanced Processing Techniques—Particulate Materials, *Proceedings Conf. on Powder Metallurgy and Particulate Materials* (Toronto), Metal Powder Industries Federation 6, 1994, p 199-210
22. Association des Usagers del Action Développement et Etudes de Procédés (ADEP), Laboratoire de Materiaux Ceramiques et Traitments de Surface at Université de Limoges, 1996
23. P. Bengtsson, " Microstructure, Residual Stress, and Thermal Shock Studies of Plasma Sprayed ZrO_2-Based Thermal Barrier Coatings," Ph.D. thesis, No. 509, Linköping University, Sweden, 1997